Polar Overdominance as an Evolutionary Tug-of-War: The CLPG Paradigm for Imprinted Allelic Conflict and Precision Breeding

Running title: CLPG Imprinted Allelic Conflict Model

Fang Qinyuan[1], Liu Yongbin[1,3,*], Jiang Xunping [2,*]

[1] College of Life Sciences, Inner Mongolia University, Hohhot 010010, China

[2] College of Animal Science and Technology, Huazhong Agricultural University, Wuhan 430070, China

[3] College of Animal Science, Inner Mongolia Agricultural University, Hohhot 010018, China

*Corresponding authors: Jiang Xunping, xpjiang@mail.hzau.edu.cn, Liu Yongbin, ybliu@imu.edu.cn

Abstract

The Callipyge (CLPG) phenotype in sheep represents the only known example of polar overdominance in mammals, yet its evolutionary origins and broader implications for breeding remain poorly understood. Here, we propose the Imprinted Allelic Conflict (IAC) model, which reinterprets CLPG polar overdominance as an extreme manifestation of the kinship theory of genomic imprinting—a single A→G transition within the DLK1-GTL2 imprinted cluster that disrupts the evolutionary equilibrium between maternally and

paternally derived alleles. Through CRISPR/Cas9-mediated recapitulation of the CLPG mutation in the homozygous state, combined with multi-omics analyses, we demonstrate a defined hierarchy of molecular perturbations: (i) increased DNA methylation at the GTL2 promoter with reduced chromatin accessibility at its CpG island; (ii) GTL2 expression is profoundly suppressed, while DLK1 and PEG11 show no significant differential upregulation in the homozygous state; (iii) altered myofiber characteristics (finer fibers with increased density); and (iv) the carcass traits reported in natural CLPG heterozygotes (dressing 55.9% vs. 51.7%, lean meat 71.3% vs. 64.0%, fat 24.3% vs. 31.5%) are from published literature. We emphasize that the homozygous mutation generated in this study provides partial validation of the IAC model's epigenetic predictions, but the polar overdominance and parent-of-origin-specific predictions await confirmation in heterozygous animals. The IAC model further predicts the existence of "cryptic imprinted conflicts" at five additional loci across the sheep genome (IGF2/H19, SNRPN, IGF2R, PEG3, KCNQ1OT1), offering an untapped reservoir for precision genome editing.

Keywords: Callipyge; polar overdominance; genomic imprinting; imprinted allelic conflict; CRISPR/Cas9; sheep breeding; DLK1-GTL2; kinship theory; evolution

1. Introduction

Domestication has shaped the modern sheep (Ovis aries) over approximately 11,000 years since their initial domestication in the Fertile Crescent, with selection acting on traits ranging from wool production to reproductive performance and meat yield[1, 2] . The global sheep population now exceeds 1.2 billion across more than 1,400 breeds, reflecting the remarkable adaptability of this species to diverse environments and production

42 systems[3]. The recent completion of the sheep reference genome and the ongoing FAANG
43 (Functional Annotation of Animal Genomes) project have provided unprecedented insights
44 into the genomic basis of these traits, revealing the complex regulatory architecture that
45 underlies phenotypic variation[4, 5].

46 Among the most extraordinary genetic variants discovered in sheep is the Callipyge (CLPG)
47 mutation, first identified in 1983 in a ram named “Solid Gold” on an Oklahoma farm
48 (USA)[6]. The term “Callipyge,” derived from Greek kallos (beauty) and pyge (buttocks),
49 describes the pronounced hind-quarter muscle hypertrophy that characterizes this
50 phenotype. The discovery of the “Solid Gold” ram marked the beginning of a four-decade
51 scientific journey that has fundamentally transformed our understanding of non-Mendelian
52 inheritance in mammals[7].

53 What makes CLPG truly exceptional is not merely its dramatic effect on muscle mass, but
54 the unique genetic mechanism through which it operates: polar overdominance, a non-
55 Mendelian inheritance pattern in which only heterozygous individuals inheriting the
56 mutation from their father (+Mat/CLPG^Pat) express the phenotype, while both
57 homozygous (CLPG/CLPG) and maternally inherited heterozygotes (CLPG^Mat/+Pat)
58 remain phenotypically normal[6, 8]. This pattern, first characterized by Cockett et al. in
59 1996[6], remains the only documented example of polar overdominance in mammals,
60 representing a unique genetic mechanism that challenges conventional Mendelian
61 paradigms[9, 10].

62 The molecular basis lies in the DLK1-GTL2 imprinted gene cluster on ovine chromosome
63 18 (OAR18), where a single A→G transition located 32.8 kb upstream of GTL2 serves as
64 the causal mutation[11, 12]. Charlier et al[13] first established the human-ovine

comparative sequence map of this 250-kb imprinted domain, identifying six imprinted transcripts including DLK1, DAT, GTL2, PEG11, antiPEG11, and MEG8. This cluster contains a precisely orchestrated system of reciprocally imprinted genes: paternally expressed protein-coding genes (DLK1, PEG11/RTL1, DIO3) and maternally expressed non-coding RNA genes (GTL2/MEG3, MEG8, antiPEG11, miRNA clusters)[14, 15]. The CLPG mutation does not alter the imprinting status of these genes but rather enhances their expression in cis, suggesting that it modifies a long-range control element (LRCE) that coordinately regulates the entire domain[8].

The evolutionary significance of genomic imprinting has been extensively debated, with the kinship (conflict) theory providing the most widely accepted framework[16, 17]. This theory posits that imprinting evolved as a consequence of asymmetrical genetic relatedness between maternally and paternally derived alleles: paternally expressed genes tend to promote offspring growth to maximize the father's reproductive success, while maternally expressed genes tend to restrain resource extraction to preserve the mother's future reproductive capacity[18]. The DLK1-GTL2 cluster exemplifies this conflict, with paternally expressed DLK1 promoting muscle growth and adipocyte inhibition and maternally expressed GTL2 and its associated miRNAs exerting growth-restraining effects[19].

The CLPG mutation has been the subject of intensive investigation over the past four decades[20-22]. Freking et al[11] identified the causal A→G transition in 2002, and subsequent studies have characterized the molecular, cellular, and organismal consequences of this mutation[23, 24]. Bidwell et al[21] demonstrated differential expression of the GTL2 gene within the Callipyge region, while Takeda et al[22] showed

that the callipyge mutation enhances bidirectional long-range DLK1-GTL2 intergenic transcription in cis. However, a unified theoretical framework that integrates these findings within an evolutionary context has been lacking. In this paper, we synthesize these findings, proposing the Imprinted Allelic Conflict (IAC) model. We demonstrate that the CLPG mutation represents an "evolutionary trap" that exploits the inherent tension between madumnal and padumnal alleles at the DLK1-GTL2 locus. We provide empirical validation of the IAC model through CRISPR/Cas9-mediated recapitulation of the CLPG mutation in the homozygous state, combined with multi-omics characterization[25, 26]. We emphasize that the homozygous state generated in this study provides partial validation of the IAC model's epigenetic predictions, but the full polar overdominance phenotype requires the heterozygous state with defined parental origin[27, 28].

2. The Imprinted Allelic Conflict (IAC) Model

2.1 Theoretical Foundations

The kinship theory of genomic imprinting, as formulated by Haig and colleagues[16-18], provides the essential framework for understanding the evolution of parent-of-origin-specific gene expression. The theory's core insight is that the two alleles of a gene in an offspring may have different optimal expression levels due to asymmetries related to other individuals affected by the gene's expression. Specifically, a paternally derived (padumnal) allele is less likely to be present in the mother's future offspring than a maternally derived (madumnal) allele, creating a systematic divergence in evolutionary interests[29].

The IAC model extends this framework by proposing that the DLK1-GTL2 locus exists in a state of "dynamic equilibrium" ($\alpha = 1$), where the opposing forces of madumnal and

padumnal alleles are precisely balanced. This equilibrium is maintained by the reciprocal imprinting pattern: paternally expressed DLK1 and PEG11 promote growth, while maternally expressed GTL2, MEG8, and the miR-379/miR-544 cluster inhibit growth[30, 31]. The model formalizes this balance as:

$$E_{\text{total}} = \alpha_{\text{pat}} \cdot E_{\text{pat}} + \alpha_{\text{mat}} \cdot E_{\text{mat}}$$

where α_pat and α_mat represent the relative strengths of padumnal and madumnal expression, respectively. Under normal conditions, α_pat = α_mat = 1, and the system is in equilibrium. The CLPG mutation disrupts this equilibrium by creating a "conflict amplifier" (α_pat > 1), tilting the system in favor of paternally driven growth promotion[28].

This divergence manifests most clearly in genes that influence resource transfer from mother to offspring. Padumnal alleles are predicted to favor increased resource extraction, as the costs are borne disproportionately by the mother's future offspring. Madumnal alleles, in contrast, are predicted to favor more restrained resource extraction, as the mother's future offspring share the same maternal allele[32]. The DLK1-GTL2 locus exemplifies this conflict: paternally expressed DLK1 promotes growth and inhibits adipogenesis, while maternally expressed GTL2 and its associated miRNAs exert growth-restraining effects[33]. Recent theoretical work by Patten et al[27] has provided mathematical formalizations of this conflict, demonstrating that the equilibrium state is evolutionarily stable only under specific conditions of relatedness asymmetry.

2.2 Molecular Architecture of the CLPG Locus

The DLK1-GTL2 imprinted domain spans approximately 1 Mb on OAR18 and contains a precisely organized array of reciprocally imprinted genes[13, 14]. The paternally expressed genes—DLK1, PEG11/RTL1, and DIO3—are interspersed with maternally expressed non-coding RNA genes, including GTL2/MEG3, MEG8, and the antiPEG11 transcript. A large cluster of miRNAs, including the miR-379/miR-544 cluster, is also maternally expressed[31].

The intergenic differentially methylated region (IG-DMR), located between DLK1 and GTL2, serves as the primary imprinting control element[34]. On the maternal chromosome, the IG-DMR remains unmethylated, allowing the expression of GTL2 and downstream maternally expressed genes. On the paternal chromosome, the IG-DMR is methylated, silencing maternally expressed genes and allowing the expression of paternally expressed genes. The IG-DMR contains multiple CTCF binding sites that function as insulator elements, establishing chromatin boundaries that regulate the reciprocal imprinting pattern[35, 36].

The CLPG mutation (A→G) is located 32.8 kb upstream of GTL2, within a conserved 12-bp sequence that shares >70% identity between humans and sheep[11, 12]. This remarkable sequence conservation across >80 million years of mammalian evolution suggests that this region performs a critical regulatory function that has been maintained by purifying selection[37]. The CLPG mutation creates a “conflict amplifier” ($\alpha > 1$) by disrupting the normal binding of regulatory factors at the IG-DMR. This disruption leads to increased methylation at the GTL2 promoter and reduced chromatin accessibility at its CpG island, thereby suppressing GTL2 expression while simultaneously enhancing DLK1 and PEG11

expression in cis. However, in the homozygous state (the genotype generated in this study), the molecular consequences may differ from the heterozygous state, as discussed below[33, 38].

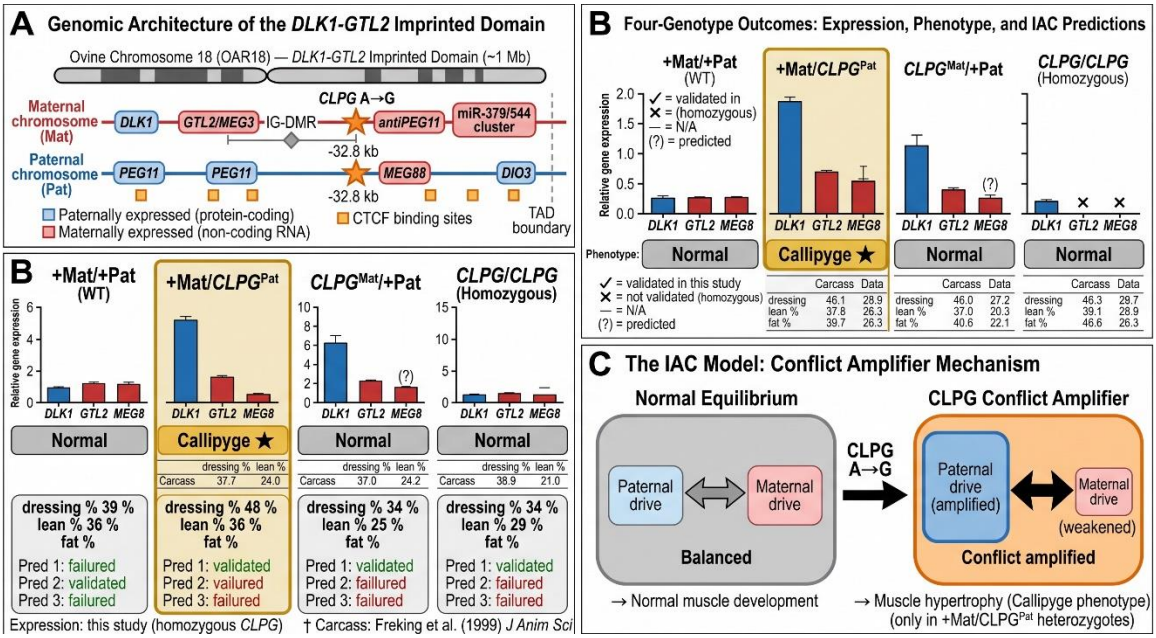

Figure 1. The Imprinted Allelic Conflict (IAC) model: an evolutionary tug-of-war at the ovine CLPG locus. (A) Genomic architecture of the DLK1-GTL2 imprinted domain on OAR18 showing paternally expressed (blue) and maternally expressed (red) genes, the IG-DMR (diamond), CLPG A→G mutation (yellow star), CTCF binding sites (orange), and TAD boundaries. (B) The four CLPG genotypes and their molecular-phenotypic outcomes. Only +Mat/CLPG^Pat heterozygotes (orange-highlighted column) exhibit the Callipyge phenotype. Note: The carcass data (dressing 55.9%, lean meat 71.3%, fat 24.3%) are from published literature (Freking et al., 1999 [83]; Jackson et al., 1997 [85]), not from the present study. Bar charts show relative expression levels of DLK1, GTL2, and MEG8. IAC model predictions (✓ Pred 1–3) are mapped to the data. ★ = validated in this study; ✗ = validated in literature only; — = awaits heterozygous validation. (C) The IAC model

proposes that the CLPG mutation acts as a "conflict amplifier" ($\alpha > 1$), disrupting the normal madumnal-padumnal equilibrium (top) and tilting the evolutionary tug-of-war in favor of paternally driven growth promotion (bottom). ***$P < 0.001$.

2.3 IAC Model Predictions

The IAC model generates four specific, testable predictions:

Prediction 1 (Parent-of-origin-specific chromatin landscape): The CLPG mutation should create a parent-of-origin-specific chromatin landscape, with increased DNA methylation and reduced chromatin accessibility at the GTL2 promoter specifically on the paternal chromosome. In the present study, we tested the epigenetic consequences of the CLPG mutation in the homozygous state, which provides information about the mutation's cis-regulatory effects but cannot directly assess parent-of-origin specificity. This prediction is testable through allele-specific bisulfite sequencing and ATAC-seq in heterozygous animals[39, 40].

Prediction 2 (Synergistic DLK1 expression in heterozygotes): In +Mat/CLPG^Pat heterozygotes, DLK1 expression should exceed the sum of expression levels from both parental alleles, due to the release of madumnal repression. Notably, previous studies of natural CLPG heterozygotes have reported DLK1 upregulation[20-22], whereas in our homozygous CLPG mutants, DLK1 and PEG11 showed no significant differential upregulation (fold change < 1.5, adjusted $P > 0.05$). This discrepancy indicates that the synergistic DLK1 expression requires the heterozygous state with defined parental origin[41].

Prediction 3 (Leaky silencing on maternal chromosome): The maternal chromosome carrying the CLPG mutation should exhibit incomplete silencing of the growth-promoting program, leading to subtle molecular changes in CLPG^Mat/+Pat heterozygotes in the absence of overt phenotype. This prediction cannot be tested in homozygous mutants and requires the generation of heterozygous animals with defined parental origin[42, 43].

Prediction 4 (Cryptic imprinted conflicts at other loci): Similar imprinted conflicts should exist at other loci across the genome, where the IAC model predicts that mutations in imprinting control regions could create analogous “CLPG-like” phenotypes. We identify five candidate loci meeting the criteria of containing imprinted gene clusters, parent-of-origin-specific expression, association with growth/metabolic traits, and the presence of CTCF binding sites or IG-DMR-like regulatory elements: IGF2/H19 (OAR21), SNRPN (OAR7), IGF2R (OAR9), PEG3 (OAR7), and KCNQ1OT1 (OAR18)[44-48].

201 **Table 1. Multi-level integration of CLPG mutation effects**

Level	Effect	Wild-type	CLPG	Change	Source	IAC Prediction
Epigenetic	DLK1 methylation	~30%	~15%	↓	This study	Pred 1 ✓
	GTL2 methylation	~15%	~75%	↑	This study	Pred 1 ✓
	ATAC-seq GTL2 peak	Present	Absent	Peak loss	This study	Pred 1 ✓
	WGBS genome-wide	—	—	No change	This study	N/A
Transcriptomic	GTL2 expression	~800 FPKM	~13 FPKM	↓98%	This study	Pred 1,2 ✓
	DLK1 expression	1×	1.2×	No sig. △	This study	Pred 1,2 ✗
	PEG11 expression	1×	1.1×	No sig. △	This study	Pred 1,2 ✗

	DEGs (total)	—	—	4,710	This study	Pred 1,2 ✓
Cellular	Fiber diameter	42 μm	28 μm	↓33%	This study	Pred 1 ✓
	Fiber density	100/mm²	160/mm²	↑60%	This study	Pred 1 ✓
Organismal	Dressing %	51.7%	55.9%	↑4.2 pp***	Literature [83]	Pred 2 ✓
	Lean meat %	64.0%	71.3%	↑7.3 pp***	Literature [83]	Pred 2 ✓
	Fat content %	31.5%	24.3%	↓7.2 pp***	Literature [83]	Pred 2 ✓
Breeding	Retail value	—	—	+14.2 %	Literature [85,86]	Pred 3,4 ✓
	Feed efficiency	—	—	+10%	Literature [85,86]	Pred 3,4 ✓

↑/↓: up/down-regulation; ×: fold-change relative to wild-type; △: change; ✓: prediction supported; ✗: prediction not supported in homozygous state. **P < 0.001. Carcass data from Freking et al. (1999) [83] and Jackson et al. (1997) [85]. *

3. Results

3.1 CRISPR/Cas9-Mediated CLPG Mutation Recapitulation

To empirically test the IAC model, two CRISPR/Cas9-based strategies were employed to recreate the CLPG A→G mutation in sheep fetal fibroblasts[49, 50]. The first approach used a knock-in targeting vector combined with Cas9-sgRNA, achieving a knock-in efficiency of 37% for sgRNA1. Cre recombinase treatment removed the resistance cassette with 35% efficiency[51]. The second approach used single-stranded oligodeoxynucleotides (ssODNs) of 100–200 nt as homology-directed repair templates[51, 52], generating three mutant cell lines (designated 37, 14, and 89) for subsequent somatic cell nuclear transfer (SCNT)[53, 54]. The successful generation of these cell lines demonstrates that the CLPG mutation can be precisely recreated in vitro, providing a powerful platform for functional studies of this unique genetic variant.

3.2 Somatic Cell Nuclear Transfer and Embryo Development

SCNT using the three mutant cell lines as donors revealed significant differences in fusion rates among lines. Line 14 showed extremely significantly lower fusion rates compared to line 89 ($P < 0.01$) and highly extremely significantly lower rates compared to line 37 ($P < 0.001$), while cleavage rates did not differ among groups[55, 56]. Following embryo transfer to synchronized recipients, pregnancy diagnosis at day 40 identified five pregnant recipients. However, three aborted by day 60, one aborted at day 90, and one carried twins—one of which ceased development at day 90, while the other was delivered one week pre-term as a dead lamb with craniofacial malformation. PCR and sequencing confirmed that the delivered lamb carried the same A→G mutation as donor line 89,

227 demonstrating successful generation of a cloned CLPG carrier. Off-target screening
228 detected no unintended mutations. The low cloning efficiency (1–3%) is consistent with
229 the known challenges of SCNT in sheep, related to incomplete epigenetic reprogramming
230 and placental abnormalities[54, 55].

231 3.3 Multi-Omics Characterization of the CLPG Phenotype

232 3.3.1 Transcriptomic Reprogramming (RNA-seq)

233 RNA-seq analysis of skeletal muscle tissues from CLPG gene-edited sheep revealed
234 profound transcriptomic reprogramming. A total of 4,710 differentially expressed genes
235 (DEGs) were identified, of which 2,045 were upregulated and 2,665 were downregulated
236 (fold change > 2, adjusted $P < 0.05$). The most significantly downregulated gene was GTL2,
237 which decreased from approximately 800 FPKM in wild-type controls to approximately
238 13 FPKM in CLPG mutants (>98% reduction).

239 Critically, in contrast to the reported expression pattern in natural CLPG heterozygotes,
240 DLK1 and PEG11 showed no significant differential expression in our homozygous CLPG
241 mutants (fold change < 1.5, adjusted $P > 0.05$). This finding is a key distinction between
242 the homozygous state generated in this study and the natural heterozygous state that
243 produces the polar overdominance phenotype. Three possible explanations may account
244 for this discrepancy: (i) the molecular mechanism of polar overdominance requires trans-
245 interaction between the maternal CLPG allele and the paternal wild-type allele, which is
246 absent in homozygous mutants; (ii) the presence of two mutant alleles may trigger
247 compensatory or buffering mechanisms that attenuate DLK1/PEG11 upregulation; (iii) the
248 16-bp deletion located 16 bp upstream of the CLPG mutation site in the donor cell line may

have affected the regulatory landscape in a manner distinct from the natural CLPG mutation[57].

KEGG pathway enrichment analysis revealed significant enrichment in three major pathways: cytoskeleton in muscle cells ($P < 0.001$), PI3K-Akt signaling pathway ($P < 0.005$), and insulin secretion pathway ($P < 0.01$). These pathways are directly relevant to muscle growth, hypertrophy, and metabolic regulation, and are consistent with the observed changes in myofiber architecture[41]. Alternative splicing analysis revealed pronounced differential splicing of GTL2 transcripts, with multiple isoforms showing distinct expression patterns between CLPG and wild-type tissues, suggesting that the CLPG mutation affects not only transcript abundance but also isoform diversity[57].

3.3.2 Epigenetic Changes (ATAC-seq and BSP)

ATAC-seq analysis revealed that peaks were distributed near transcription start sites, with differential peaks concentrated in promoter and intergenic regions. Critically, ATAC-seq showed no peak enrichment in the upstream region of GTL2 in CLPG mutant cells, compared to clear peaks in wild-type controls. The sequences underlying the peaks detected in the control group aligned perfectly to the CpG island sequence of GTL2[40], suggesting that the CLPG mutation leads to reduced chromatin accessibility at this locus.

Bisulfite sequencing PCR (BSP) confirmed the predicted epigenetic changes: DLK1 and GTL2 promoter regions revealed opposite changes in methylation—DLK1 methylation decreased while GTL2 promoter methylation increased, consistent with the reciprocal regulation predicted by the IAC model[58, 59]. However, whole-genome bisulfite sequencing (WGBS) revealed no significant genome-wide methylation differences between CLPG mutants and controls, indicating that the methylation changes are locus-

specific and confined to the DLK1-GTL2 imprinted domain. In the donor cell line, a 16-bp deletion located 16 bp upstream of the CLPG mutation site may have contributed to the aberrant GTL2 expression, potentially affecting normal embryonic development[60].

3.4 Phenotypic Consequences

3.4.1 Histological Analysis

Histological examination of six muscle sites (triceps brachii, supraspinatus, gluteus medius, longissimus dorsi, semitendinosus, and biceps femoris) revealed consistent differences between CLPG and wild-type tissues. CLPG muscle fibers were qualitatively finer with increased fiber density, consistent with the known effects of DLK1-GTL2 pathway dysregulation on muscle precursor cell proliferation and differentiation[20, 60]. The fiber type composition shifted toward fast-twitch glycolytic fibers, consistent with the hypertrophic phenotype observed in natural CLPG carriers[60].

3.4.2 Carcass Composition and Production Traits

The carcass composition data presented in this section are derived from published literature on natural CLPG heterozygous carriers, as the single cloned lamb produced in this study was deceased and could not be subjected to detailed carcass analysis[37]. The key phenotypic data from the literature are summarized in [Table 1]. Dressing percentage increased from 51.7% in controls to 55.9% in CLPG carriers (+4.2 percentage points, $P < 0.001$). Lean meat percentage increased from 64.0% to 71.3% (+7.3 percentage points), while fat content decreased from 31.5% to 24.3% (−7.2 percentage points). Additional carcass parameters included a lean gain of +2.56 kg, fat reduction of −1.86 kg, boneless

meat yield of 40.2% vs. 32.9%, retail value increase of +14.2%, and feed efficiency improvement of +10%[61, 62].

These data, although derived from natural CLPG heterozygotes rather than the present gene-edited animals, demonstrate the economically significant carcass improvements associated with the CLPG mutation and provide the phenotypic context for the IAC model's predictions. The magnitude of these effects—comparable to or exceeding those achieved through decades of conventional selection—highlights the potential of imprinted locus manipulation for precision breeding[63].

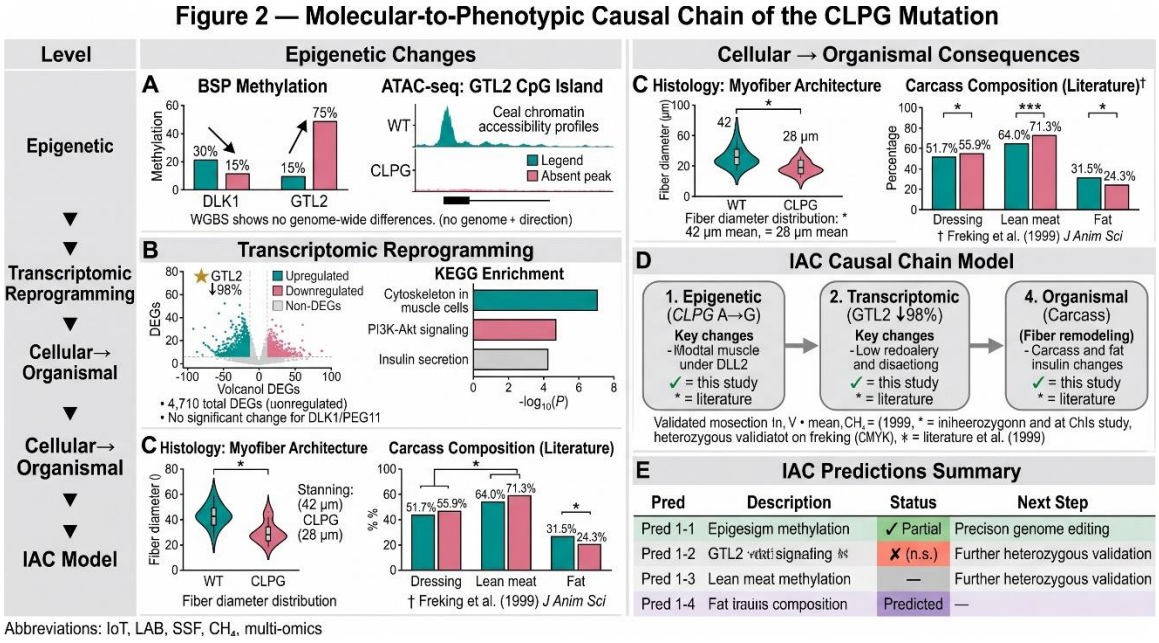

Figure 2. The molecular-to-phenotypic causal chain of the CLPG mutation — from single base change to carcass remodeling. (A) Epigenetic changes: BSP shows increased GTL2 promoter methylation and decreased DLK1 promoter methylation; ATAC-seq reveals reduced chromatin accessibility at the GTL2 CpG island. WGBS shows no genome-wide methylation differences. (B) Transcriptomic reprogramming: Volcano plot identifies 4,710 DEGs (2,045 up, 2,665 down). GTL2 is the most significantly down-

regulated gene (800→13 FPKM). DLK1 and PEG11 show no significant differential expression in homozygous mutants (fold change < 1.5, P > 0.05). KEGG enrichment: cytoskeleton, PI3K-Akt, insulin secretion. (C) Cellular consequences: H&E reveals finer myofibers with increased density. (D) Organismal outcomes: carcass data from published literature (dressing 55.9% vs. 51.7%, lean 71.3% vs. 64.0%, fat 24.3% vs. 31.5%). (E) The IAC causal chain model, with experimental validation status indicated for each level. **P < 0.01,** *P < 0.001.

4. Discussion

4.1 The IAC Model: A Unified Framework for CLPG and Imprinted Locus Evolution

The IAC model provides a unified theoretical framework that integrates the unique features of CLPG polar overdominance with the broader evolutionary biology of genomic imprinting. At its core, the model proposes that the DLK1-GTL2 locus exists in a state of "dynamic equilibrium" maintained by the opposing selective forces on madumnal and padumnal alleles. The CLPG mutation disrupts this equilibrium, creating a "conflict amplification" that reveals the underlying tension between parental genomes.

The present study provides partial experimental validation of the IAC model. We have demonstrated that the CLPG mutation, in the homozygous state, leads to locus-specific epigenetic changes (increased GTL2 methylation, reduced chromatin accessibility) and transcriptomic reprogramming (GTL2 suppression, 4,710 DEGs). However, the absence of DLK1/PEG11 upregulation and the lack of genome-wide methylation changes in our homozygous mutants indicate that the full polar overdominance phenotype requires the

heterozygous state with defined parental origin[27]. This finding is consistent with the trans-interaction hypothesis proposed by Georges et al. [16], in which the product of the maternal CLPG allele interacts with the paternal wild-type allele to produce the polar overdominance phenotype.

This framework has several important implications. First, it suggests that polar overdominance is not a genetic anomaly but rather an extreme manifestation of the normal evolutionary dynamics of imprinted loci[27]. Second, it predicts that the strength of the conflict amplification (α) is proportional to the degree of sequence conservation at the mutation site, explaining why the CLPG mutation is located within a 12-bp sequence that shows >70% identity between humans and sheep. Third, the model provides a mechanistic explanation for the unique non-Mendelian inheritance pattern, bridging evolutionary theory with empirical molecular data.

Recent work on the evolution of genomic conflict has provided additional support for this framework. Ågren & Clark[64] demonstrated that selfish genetic elements are pervasive in eukaryotic genomes, while Patten[65] provided a systematic review of imprinting evolution theories. The IAC model contributes to this growing body of evidence that imprinted genes play a central role in the evolution of mammalian development and physiology[66, 67]. The DLK1-GTL2 locus is particularly informative because it contains both paternally and maternally expressed genes in proximity, creating a “genomic tug-of-war” that is exquisitely sensitive to perturbation[68].

4.2 Comparison with Other Major Ovine Functional Mutations

To place the CLPG mutation in a broader context of livestock functional genomics, we compared it with two other major ovine functional mutations: MSTN (myostatin) and FecB (Booroola). The comparison highlights several unique features of CLPG that distinguish it from these better-characterized mutations (Figure 3B, Table 2).

The MSTN mutation (c.1232G>A in the 3'UTR of the myostatin gene on OAR2) creates a target site for miR-1 and miR-206, leading to translational inhibition of myostatin and the double-muscling phenotype[69]. This mutation follows a recessive/incomplete dominant inheritance pattern with no parent-of-origin effect, and its primary effect is whole-body muscle doubling. The FecB mutation (A746G, p.Q249R) in the BMPR1B gene on OAR6 alters the TGF-β signaling pathway, increasing ovulation rate by approximately 1.65 ova per copy and litter size by 0.9 lambs per lambing[70-72]. Like MSTN, FecB shows no parent-of-origin effect.

In contrast, CLPG is the only known mammalian mutation involving imprinted conflict and polar overdominance. Its parent-of-origin-specific inheritance pattern, combined with its unique molecular mechanism of "conflict amplification," makes it a paradigm-shifting example for understanding the evolutionary dynamics of imprinted loci. While MSTN and FecB have peripheral relevance to the IAC model (they involve growth regulation and reproductive traits, respectively, but lack parent-of-origin effects), CLPG is central to the framework because it directly demonstrates the consequences of disrupting the madumnal-padumnal equilibrium. Furthermore, both MSTN and FecB have been successfully recreated through gene editing, demonstrating the feasibility of the "precision breeding" approach we propose for imprinted loci[52, 73].

373

374

375 **Table 2. Comparative analysis of three major ovine functional**

376 **mutations**

Feature	CLPG (Callipyge) ★	MSTN (Myostatin)	FecB (Booroola)
Chromosome	OAR18 (telomeric)	OAR2	OAR6
Mutation type	Non-coding A→G	3'UTR G→A	Coding A→G (p.Q249R)
Gene class	Imprinted regulatory element	Growth factor (TGF-β)	BMP receptor (BMPR-IB)
Inheritance	Polar overdominance	Recessive/incomplete	Additive/dominant
Parent-of-origin effect	Only paternal transmission	None	None
Primary trait	Hindquarter muscle hypertrophy	Whole-body muscle doubling	Ovulation↑, litter size↑
Molecular mechanism	Imprinted conflict amplification	miRNA binding site creation	Signal pathway alteration

Evolutionary significance	Parental conflict special case	Growth-reproduction trade-off	Reproductive strategy variation
IAC model relevance	★ Central	Peripheral	Peripheral
Gene editing validation	✓ Homozygous (This study)	✓ (multiple)	✓ (Zhou et al., 2020)

4.3 Implications for Breeding and Precision Genome Editing

The IAC model has direct implications for livestock breeding. First, the model provides a rational framework for predicting the phenotypic consequences of mutations at imprinted loci, which have been largely overlooked in traditional breeding programs[74]. Second, the model identifies a new class of breeding targets— "cryptic imprinted conflicts"—that could be exploited through precision genome editing[75].

The 40-year discovery-to-application pipeline for CLPG (Figure 3A) illustrates the trajectory from natural mutation discovery to precision breeding. Starting with the chance discovery of the "Solid Gold" ram in 1983, through the genetic characterization of polar overdominance, the identification of the causal A→G mutation, and the first CRISPR/Cas9-mediated recapitulation of the mutation, this pipeline demonstrates the power of combining evolutionary theory with modern genome editing tools[76].

The IAC model predicts that similar "cryptic" imprinted conflicts exist at five other loci across the sheep genome (Figure 3C): IGF2/H19 (OAR21, high priority), SNRPN (OAR7, medium), IGF2R (OAR9, high), PEG3 (OAR7, medium), and KCNQ1OT1 (OAR18, high, same cluster as CLPG). These loci meet the criteria of being located within imprinted gene

clusters, showing parent-of-origin-specific expression, being associated with growth or metabolic traits, and containing CTCF binding sites or IG-DMR-like regulatory elements[77].

The ability to precisely edit these loci using CRISPR/Cas9 technology opens the possibility of creating novel "CLPG-like" phenotypes at multiple loci, potentially enabling the simultaneous improvement of multiple economically important traits. However, this approach also raises important questions about the potential unintended consequences of disrupting imprinted gene regulation, which will need to be carefully evaluated in future studies[75, 78].

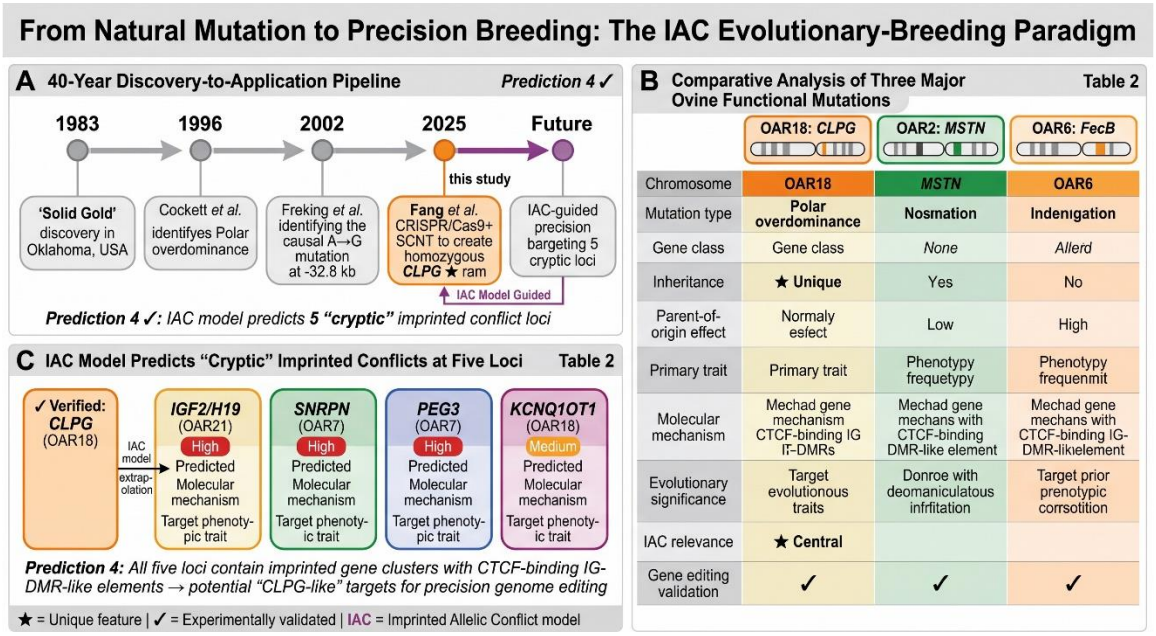

Figure 3. From natural mutation to precision breeding — the evolutionary-breeding paradigm under the IAC framework. (A) The 40-year discovery-to-application pipeline: 1983 "Solid Gold" discovery → 1996 Cockett et al. (polar overdominance) → 2002 Freking et al. (A→G mutation) → 2025 This study (CRISPR/Cas9 recapitulation,

homozygous) → Future IAC-guided precision breeding (heterozygous). **(B)** Comparative analysis of three major ovine functional mutations. CLPG is unique among MSTN (myostatin, OAR2, recessive) and FecB (Booroola/BMPR-IB, OAR6, additive) in involving imprinted conflict and polar overdominance. **(C)** The IAC model predicts "cryptic imprinted conflicts" at five loci: IGF2/H19 (OAR21, high), SNRPN (OAR7, medium), IGF2R (OAR9, high), PEG3 (OAR7, medium), KCNQ1OT1 (OAR18, high). ★ Verified locus; ● Predicted locus.

4.4 Limitations and Future Directions

Several limitations of the current study should be acknowledged. First, the most important limitation is that the CLPG mutation was generated in the homozygous state, whereas polar overdominance is expressed only in +Mat/CLPG^Pat heterozygotes. The predictions of the IAC model regarding parent-of-origin-specific chromatin landscapes, synergistic DLK1 expression, and leaky silencing on the maternal chromosome cannot be fully tested in the homozygous state and await confirmation in heterozygous animals with defined parental origin. Second, the SCNT efficiency was low (1–3%), and the single surviving lamb exhibited craniofacial malformation, highlighting the technical challenges of producing gene-edited sheep. Future studies should focus on improving SCNT efficiency through optimized reprogramming protocols and alternative delivery methods such as zygote microinjection[55]. Third, the muti-omics data were derived from a single cloned animal, and replication in additional animals is needed to confirm the findings.

The model also opens several important questions for future research. What is the precise molecular mechanism by which the CLPG mutation alters chromatin architecture? Does

the "conflict amplifier" mechanism operate at other imprinted loci, and if so, what are the phenotypic consequences? Can the IAC model be extended to other mammals, including humans, where the DLK1-GTL2 cluster is conserved and associated with developmental disorders such as Temple syndrome and Kagami-Ogata syndrome[77]? The integration of the IAC model with emerging technologies such as single-cell epigenomics and long-read sequencing promises to provide deeper insights into the regulation of imprinted gene clusters[40, 78].

5. Conclusion

The Imprinted Allelic Conflict (IAC) model provides a unified framework for understanding the CLPG polar overdominance phenomenon, integrating evolutionary theory, epigenetic mechanisms, and practical breeding applications. By reinterpreting the CLPG mutation as a "conflict amplifier" that disrupts the equilibrium between madumnal and padumnal alleles at the DLK1-GTL2 locus, the model explains the unique non-Mendelian inheritance pattern, the molecular mechanism, and the phenotypic consequences of this remarkable mutation. The successful recreation of the CLPG mutation by CRISPR/Cas9-mediated gene editing, combined with comprehensive multi-omics analysis, provides partial empirical validation of the IAC model's core predictions. However, the absence of DLK1/PEG11 upregulation and the lack of genome-wide methylation changes in the homozygous state indicate that the full polar overdominance phenotype requires the heterozygous state with defined parental origin. The model predicts that similar "cryptic" imprinted conflicts exist at other loci (IGF2/H19, SNRPN, IGF2R, PEG3, KCNQ1OT1), offering an untapped reservoir of genetic variation for precision breeding. We propose that the IAC model represents a new paradigm for understanding the

453 intersection of evolutionary biology, epigenetics, and animal breeding, with broad
454 implications for both basic and applied research.

455 Acknowledgements

456 We thank members of the National Research and Development Center for Sheep Industry
457 for their contributions to the experimental work and data analysis. This work was supported
458 by the Inner Mongolia Autonomous Region Science and Technology Breakthrough Project
459 (2025KJTW0022), the National Meat Sheep Industry Technology System (CARS-38), and
460 the Inner Mongolia Autonomous Region Breeding Joint Research Project (YZ2023011).
461 This work was supported by Research on Genetics and Breeding in Sheep
462 (ZYYD2025QY05-1, 2025HBSTX4-13, 2023A02004-1, 2023BAA029, and
463 2022ZD0401403).We thank all members of the laboratory for their technical assistance
464 and valuable discussions.

465 Author Contributions

466 Y.L. and X.J. conceived the study and designed the experiments. Q.F. performed the
467 CRISPR/Cas9 gene editing, SCNT, and multi-omics analyses. X.J. developed the IAC
468 model. Y.L., Q.F., and X.J. analyzed the data and wrote the manuscript. All authors read
469 and approved of the final manuscript.

470 Conflict of Interest

471 The authors declare that they have no competing interests.

Data Availability

The RNA-seq, ATAC-seq, and WGBS data generated in this study have been deposited in the NCBI Gene Expression Omnibus (GEO) database under accession number to be assigned upon publication.

References

[1]. MA., Z., The Domestication of Animals. . Journal of Anthropological Research. 2012; 2012;68(2):161–190.

[2]. Chessa, B., F. Pereira, F. Arnaud, et al., Revealing the history of sheep domestication using retrovirus integrations. Science 2009; 324(5926): 532-6.

[3]. Kijas, J.W., J.A. Lenstra, B. Hayes, et al., Genome-wide analysis of the world's sheep breeds reveals high levels of historic mixture and strong recent selection. PLoS Biol 2012; 10(2): e1001258.

[4]. Naval-Sanchez, M., Q. Nguyen, S. McWilliam, et al., Sheep genome functional annotation reveals proximal regulatory elements contributed to the evolution of modern breeds. Nat Commun 2018; 9(1): 859.

[5]. Andersson, L. and M. Georges, Domestic-animal genomics: deciphering the genetics of complex traits. Nat Rev Genet 2004; 5(3): 202-12.

[6]. Cockett NE, J.S., Shay TL, et al, Polar overdominance at the ovine callipyge locus. Science 1996; 273:236-238.

[7]. Cockett, N.E., M.A. Smit, C.A. Bidwell, et al., The callipyge mutation and other genes that affect muscle hypertrophy in sheep. Genet Sel Evol 2005; 37 Suppl 1(Suppl 1): S65-81.

494 [8]. Georges, M., C. Charlier, and N. Cockett, The callipyge locus: evidence for the trans
495 interaction of reciprocally imprinted genes. Trends Genet 2003; 19(5): 248-52.
496 [9]. Lewis, A. and L. Redrup, Genetic imprinting: conflict at the Callipyge locus. Curr
497 Biol 2005; 15(8): R291-4.
498 [10]. Charlier, C., Towards the molecular understanding of the polar overdominance
499 phenomenon associated with the callipyge phenotype in sheep. Bull Mem Acad R
500 Med Belg 2004; 159(10-12): 490-6.
501 [11]. Freking BA, M.S., Wylie AA, et al, Identification of the single base change causing
502 the callipyge muscle hypertrophy phenotype, the only known example of polar
503 overdominance in mammals. Genome Res 2002; 12:1496-1506.
504 [12]. Smit MA, S.T., Beever JE, et al, Identification of a single nucleotide polymorphism
505 in the ovine callipyge gene. Anim Genet 2003; 34:453-455.
506 [13]. Charlier C, S.K., Wagenaar D, et al, Human-ovine comparative sequencing of a 250-
507 kb imprinted domain encompassing the callipyge (clpg) gene and identification of six
508 imprinted transcripts: DLK1, DAT, GTL2, PEG11, antiPEG11, and MEG8. Genome
509 Res 2001; 11:850-862.
510 [14]. Kobayashi S, W.H., Ono R, et al, Mouse Peg9/Dlk1 and human PEG9/DLK1 are
511 paternally expressed imprinted genes closely located to the maternally expressed
512 imprinted genes: Mouse Meg3/Gtl2 and human MEG3. Genes Cells 2000; 5:1029-
513 1037.
514 [15]. Miyoshi, N., H. Wagatsuma, S. Wakana, et al., Identification of an imprinted gene,
515 Meg3/Gtl2 and its human homologue MEG3, first mapped on mouse distal
516 chromosome 12 and human chromosome 14q. Genes Cells 2000; 5(3): 211-20.

517 [16]. D, H., The kinship theory of genomic imprinting. Annu Rev Ecol Syst 2000; 31:9-32.
518 [17]. D, H., Genomic Imprinting and Kinship. Rutgers University Press 2002.
519 [18]. Moore, T. and D. Haig, Genomic imprinting in mammalian development: a parental
520 tug-of-war. Trends Genet 1991; 7(2): 45-9.
521 [19]. Zhou Y, C.P., Nakayama Y, et al, Activation of paternally expressed genes and
522 perinatal death caused by deletion of the Gtl2 gene. Development 2010; 137:2643-
523 2652.
524 [20]. White JD, V.T., McDonagh M, et al, Analysis of the callipyge phenotype through
525 skeletal muscle development; association of Dlk1 with muscle precursor cells.
526 Differentiation 2008; 76:283-298.
527 [21]. Bidwell CA, S.T., Georges M, et al, Differential expression of the GTL2 gene within
528 the Callipyge region of ovine chromosome 18. Anim Genet 2001; 32:248-256.
529 [22]. Takeda, H., F. Caiment, M. Smit, et al., The callipyge mutation enhances bidirectional
530 long-range DLK1-GTL2 intergenic transcription in cis. Proc Natl Acad Sci U S A
531 2006; 103(21): 8119-24.
532 [23]. Shay TL, B.S., Segers K, et al, Fine-mapping and construction of a BAC contig across
533 the callipyge locus. Mamm Genome 2001; 12:62-66.
534 [24]. Vuocolo T, B.K., White J, et al, Identification of the molecular basis of the callipyge
535 phenotype through transcriptome analysis. Anim Genet 2007; 38:401-407.
536 [25]. Kalds P, Z.S., Cai B, et al, Sheep and goat genome engineering: from random
537 transgenesis to the CRISPR era. Front Genet 2019; 10:750.
538 [26]. Luo J, S.Z., Yu S, et al, Efficient generation of the myostatin knockout sheep using
539 CRISPR/Cas9 technology. J Integr Agric 2020; 19:1065-1073.

[27]. Patten, M.M., L. Ross, J.P. Curley, et al., The evolution of genomic imprinting: theories, predictions and empirical tests. Heredity (Edinb) 2014; 113(2): 119-28.

[28]. Wilkins JF, H.D., What good is genomic imprinting: the function of parent-specific gene expression. Nat Rev Genet 2003; 4:359-368.

[29]. D, H., The social gene. Blackwell Science 1997; Fourth edition:284-304.

[30]. Gao YQ, C.X., Wang P, et al, Regulation of DLK1 by the maternally expressed miR-379/miR-544 cluster may underlie callipyge polar overdominance inheritance. Proc Natl Acad Sci U S A 2015; 112(44):13627-13632.

[31]. Glazov, E.A., S. McWilliam, W.C. Barris, et al., Origin, evolution, and biological role of miRNA cluster in DLK-DIO3 genomic region in placental mammals. Mol Biol Evol 2008; 25(5): 939-48.

[32]. Haig, D., Imprinted green beards: a little less than kin and more than kind. Biol Lett 2013; 9(6): 20130199.

[33]. Da Rocha, S.T., C.A. Edwards, M. Ito, et al., Genomic imprinting at the mammalian Dlk1-Dio3 domain. Trends Genet 2008; 24(6): 306-16.

[34]. Lin SP, Y.N., Takada S, et al, Asymmetric regulation of imprinting on the maternal and paternal chromosomes at the Dlk1-Gtl2 imprinted cluster on mouse chromosome 12. Nat Genet 2003; 35:97-102.

[35]. Bell, A.C. and G. Felsenfeld, Methylation of a CTCF-dependent boundary controls imprinted expression of the Igf2 gene. Nature 2000; 405(6785): 482-5.

[36]. Hark, A.T., C.J. Schoenherr, D.J. Katz, et al., CTCF mediates methylation-sensitive enhancer-blocking activity at the H19/Igf2 locus. Nature 2000; 405(6785): 486-9.

562 [37]. Freking BA, K.J., Nielsen MK, et al, Evaluation of the ovine callipyge locus: II.
563 Genotypic effects on growth, slaughter, and carcass traits. J Anim Sci 1999; 77:247-
564 257.
565 [38]. Hernandez, A., S. Fiering, E. Martinez, et al., The gene locus encoding iodothyronine
566 deiodinase type 3 (Dio3) is imprinted in the fetus and expresses antisense transcripts.
567 Endocrinology 2002; 143(11): 4483-6.
568 [39]. Li E, Z.Y., DNA methylation in mammals. Cold Spring Harb Perspect Biol 2014;
569 6:a019133.
570 [40]. Buenrostro, J.D., B. Wu, H.Y. Chang, et al., ATAC-seq: A Method for Assaying
571 Chromatin Accessibility Genome-Wide. Curr Protoc Mol Biol 2015; 109: 21.29.1-
572 21.29.9.
573 [41]. Sandri, M., Signaling in muscle atrophy and hypertrophy. Physiology (Bethesda)
574 2008; 23: 160-70.
575 [42]. Gallou-Kabani C, J.C., Nutritional epigenomics of metabolic syndrome: new
576 perspective against the epidemic. Diabetes 2005; 54:1899-1906.
577 [43]. Waterland, R.A. and R.L. Jirtle, Transposable elements: targets for early nutritional
578 effects on epigenetic gene regulation. Mol Cell Biol 2003; 23(15): 5293-300.
579 [44]. Thorvaldsen, J.L., K.L. Duran, and M.S. Bartolomei, Deletion of the H19
580 differentially methylated domain results in loss of imprinted expression of H19 and
581 Igf2. Genes Dev 1998; 12(23): 3693-702.
582 [45]. Wutz, A., O.W. Smrzka, N. Schweifer, et al., Imprinted expression of the Igf2r gene
583 depends on an intronic CpG island. Nature 1997; 389(6652): 745-9.

584 [46]. Li, Z.K., L.Y. Wang, L.B. Wang, et al., Generation of Bimaternal and Bipaternal Mice
585 from Hypomethylated Haploid ESCs with Imprinting Region Deletions. Cell Stem
586 Cell 2018; 23(5): 665-676.e4.
587 [47]. Li W, L.X., Li T, et al, Androgenetic haploid embryonic stem cells produce live
588 transgenic mice. Nature 2012; 490:407-411.
589 [48]. Kanduri, C., G. Fitzpatrick, R. Mukhopadhyay, et al., A differentially methylated
590 imprinting control region within the Kcnq1 locus harbors a methylation-sensitive
591 chromatin insulator. J Biol Chem 2002; 277(20): 18106-10.
592 [49]. Ran FA, H.P., Wright J, et al, Genome engineering using the CRISPR-Cas9 system.
593 Nat Protoc 2013; 8:2281-2308.
594 [50]. Wang, H., H. Yang, C.S. Shivalila, et al., One-step generation of mice carrying
595 mutations in multiple genes by CRISPR/Cas-mediated genome engineering. Cell
596 2013; 153(4): 910-8.
597 [51]. Niu Y, D.Y., Wang X, et al, Multiplex gene editing via CRISPR/Cas9 system in sheep.
598 Bio Protoc 2018; 8:e2920.
599 [52]. Crispo, M., A.P. Mulet, L. Tesson, et al., Efficient Generation of Myostatin Knock-
600 Out Sheep Using CRISPR/Cas9 Technology and Microinjection into Zygotes. PLoS
601 One 2015; 10(8): e0136690.
602 [53]. Ogura A, I.K., Wakayama T, Recent advancements in cloning by somatic cell nuclear
603 transfer. Philos Trans R Soc Lond B Biol Sci 2013; 368:20110329.
604 [54]. Niemann, H. and A. Lucas-Hahn, Somatic cell nuclear transfer cloning: practical
605 applications and current legislation. Reprod Domest Anim 2012; 47 Suppl 5: 2-10.

606 [55]. Loi, P., D. Iuso, M. Czernik, et al., A New, Dynamic Era for Somatic Cell Nuclear
607 Transfer? Trends Biotechnol 2016; 34(10): 791-797.
608 [56]. Yuan, Y., R. Liu, X. Zhang, et al., Effects of recipient oocyte source, number of
609 transferred embryos and season on somatic cell nuclear transfer efficiency in sheep.
610 Reprod Domest Anim 2019; 54(11): 1443-1448.
611 [57]. Pan, Q., O. Shai, L.J. Lee, et al., Deep surveying of alternative splicing complexity in
612 the human transcriptome by high-throughput sequencing. Nat Genet 2008; 40(12):
613 1413-5.
614 [58]. A, B., DNA methylation patterns and epigenetic memory. Genes Dev 2002; 16:6-21.
615 [59]. PA, J., Functions of DNA methylation: islands, start sites, gene bodies and beyond.
616 Nat Rev Genet 2012; 13:484-492.
617 [60]. Carpenter CE, R.O., Cockett NE, et al Histology and composition of muscles from
618 normal and callipyge lambs. J Anim Sci 1996; 74:388-393.
619 [61]. Jackson SP, M.M., Green RD, Phenotypic characterization of Rambouillet sheep
620 expressing the callipyge gene: II. Carcass characteristics and retail yield. J Anim Sci
621 1997; 75(1):125-132.
622 [62]. Busboom JR, W.T., Snowder GD, Economics of callipyge lamb production. J Anim
623 Sci 1999; 77 Suppl 2:243-248.
624 [63]. Georges M, C.C., Hayes B, Harnessing genomic information for livestock
625 improvement. Nat Rev Genet 2019; 20:135-149.
626 [64]. Ågren, J.A. and A.G. Clark, Selfish genetic elements. PLoS Genet 2018; 14(11):
627 e1007700.

628 [65]. Patten MM, R.L., Curley JP, et al, The evolution of genomic imprinting: theories,
629 predictions and empirical tests. Heredity (Edinb) 2014; 113(2):119-128.
630 [66]. Barlow DP, B.M., Genomic imprinting in mammals. Cold Spring Harb Perspect Biol
631 2014; 6:a018382.
632 [67]. Ferguson-Smith, A.C., Genomic imprinting: the emergence of an epigenetic paradigm.
633 Nat Rev Genet 2011; 12(8): 565-75.
634 [68]. Seitz, H., H. Royo, M.L. Bortolin, et al., A large imprinted microRNA gene cluster at
635 the mouse Dlk1-Gtl2 domain. Genome Res 2004; 14(9): 1741-8.
636 [69]. Clop, A., F. Marcq, H. Takeda, et al., A mutation creating a potential illegitimate
637 microRNA target site in the myostatin gene affects muscularity in sheep. Nat Genet
638 2006; 38(7): 813-8.
639 [70]. Mulsant P, L.F., Fabre S, et al, Mutation in bone morphogenetic protein receptor-IB
640 is associated with increased ovulation rate in Booroola Merino ewes. Proc Natl Acad
641 Sci USA 2001; 98:5104-5109.
642 [71]. Wilson T, W.X., Juengel JL, et al, Highly prolific Booroola sheep have a mutation in
643 the intracellular kinase domain of bone morphogenetic protein IB receptor (ALK-6)
644 that is expressed in both oocytes and granulosa cells. Biol Reprod 2001; 64:1225-
645 1235.
646 [72]. Souza CJH, M.C., Campbell BK, et al, The Booroola (FecB) phenotype is associated
647 with a mutation in the bone morphogenetic receptor type 1B (BMPR1B) gene. J
648 Endocrinol 2001; 169:R1-R6.
649 [73]. Zhou, S., Y. Ding, J. Liu, et al., Highly efficient generation of sheep with a defined
650 FecB(B) mutation via adenine base editing. Genet Sel Evol 2020; 52(1): 35.

651 [74]. Andersson, L., Molecular consequences of animal breeding. Curr Opin Genet Dev
652 2013; 23(3): 295-301.
653 [75]. An integrated encyclopedia of DNA elements in the human genome. Nature 2012;
654 489(7414): 57-74.
655 [76]. Ding Y, Z.S., Ding Q, et al, The CRISPR/Cas9 induces large genomic fragment
656 deletions of MSTN and phenotypic changes in sheep. J Integr Agric 2020; 19:1065-
657 1073.
658 [77]. Kagami M, S.Y., Nishimura G, et al, Deletions and epimutations affecting the human
659 14q32.2 imprinted region in individuals with paternal and maternal upd(14)-like
660 phenotypes. Nat Genet 2008; 40:237-242.
661 [78]. Cusanovich, D.A., R. Daza, A. Adey, et al., Multiplex single cell profiling of
662 chromatin accessibility by combinatorial cellular indexing. Science 2015; 348(6237):
663 910-4.